ARTICLE IN PRESS

Ceramics International xxx (xxxx) xxx–xxx

Contents lists available at ScienceDirect

Ceramics International

journal homepage: www.elsevier.com/locate/ceramint

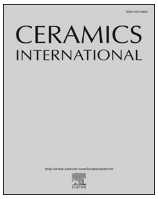

# Electrospun carbon nanofibers decorated with MnO nanoparticles as a sulfur-absorbent for lithium-sulfur batteries

Jinghui Zhu, Rosaiah Pitcheri, Tuo Kang, Ya Guo, Jing Li, Yejun Qiu*

*Shenzhen Engineering Lab of Flexible Transparent Conductive Films, Department of Materials Science and Engineering, Harbin Institute of Technology, Shenzhen 518055, China*

ARTICLE INFO

*Keywords:*
Li-S batteries
Electrospinning
MnO
Carbon nanofibers
Electrochemical properties

ABSTRACT

Shuttle effect of the dissolved polysulfide is a main disadvantage for Li-S batteries, which has been explored by several polar materials to absorb lithium polysulfide with physical and chemical effect. Herein, for the first time, a composite of carbon nanofibers decorated with MnO nanoparticles (CNF-MnO) has been prepared by the facile electrospinning method followed by thermal treatment. SEM and TEM characterization delivered that the MnO NPs on CNF did not change the morphology but decrease the electronic conductivity of CNF-MnO composite. The CNF-MnO composite exhibited excellent electrochemical cyclic stability because of its strong chemical absorption for polysulfide. Interestingly, CNF-MnO composite served as both cathode as well interlayer for Li-S batteries. The CNF-MnO-S as cathode material showed an initial discharge capacity of 683.2 mAh $g^{-1}$ at 1.0 C and remained 592.0 mAh $g^{-1}$ even after 250 cycles with the capacity decay of 0.053% per cycle. As well, CNF-MnO as interlayer delivered superior cycling stability even at high current density of 3.0 C, where the capacity still maintained 542.2 mAh $g^{-1}$ over 200 cycles.

## 1. Introduction

Among various batteries reported so far, lithium-sulfur (Li-S) batteries have received more attention on account of their high theoretical specific capacity (1675 mAh/g) and high specific energy (2600 Wh/kg), which are much higher than that of Li-ion batteries at present. Moreover, natural abundance, environmental friendliness and low cost of sulfur make it applicable for the upcoming energy material [1,2]. However, the practical performances of Li-S batteries are still limited by various hindrances. Firstly, sulfur or $Li_2S$ as the cathode material obstruct the electron conduction owing to the insulating nature. Secondly, the volume changes of sulfur cathode during cycling would cause exfoliation from the current collector. Thirdly, the discharge products of lithium polysulfides (LiPSs) are easily dissolve into the electrolyte solutions, which cause the “shuttle effect” [3–5].

In order to resolve above issues, numerous efforts have been applied to improve the performance of Li-S batteries. For instance, carbonaceous materials, such as carbon nanotubes [6,7], porous carbon [8,9], carbon spheres [10,11], carbon nanofibers [12,13] and reduced graphene oxide [14,15] are composited with sulfur to make the performance of the Li-S battery better. These carbonaceous materials not only improve the electron and Li-ion conductivity for S cathode, but also adjust the volume change and restrict the polysulfides shuttle physically with a result of their large specific surface area or pore size. However, the nature of these conventional absorbing materials is non-polar and only possesses weak interaction with the polar polysulfide via their physical absorption, which results poor cycle performance [16,17]. Therefore, several studies have focused on the fabrication of functional carbon materials with doping/ decoration of other polar materials, which is favorable to remit the shuttle effect via chemical absorption.

Currently, the carbonaceous materials are composite with the various metal oxides such as $MnO_2$ [18–20], $TiO_2$ [21,22], $Ti_4O_7$ [23,24], ZnO [25,26], MgO [27,28], $Co_3O_4$ [29,30] and $Li_4Ti_5O_{12}$ [31] etc, which can be as LiPSs chemical absorption agents, because metal oxide would enhance the absorption ability largely to entrap LiPSs compared with non-polar carbonaceous materials. Among these, MnO can not only improve the electrical conductivity but also exhibit stable electrochemical performance even at high current densities. In this study, MnO decorated carbon nanofibers (CNF-MnO) are fabricated with a facile electrospinning method and apply in Li-S batteries for the first time. CNF as a carbon matrix can form a continuous electron conductive network and improve the adhesion of S cathode. MnO NPs dispersed uniformly throughout the CNFs can restrict the LiPSs shuttle effectively between cathode and Li anode with chemical absorption. The effective combination of CNF and MnO NPs can form a new 3D conductive structure to make the Li-ion conduction convenient. As a S

---

* Corresponding author.
*E-mail addresses:* yejunqiu@hit.edu.cn, qiuyejun2016@aliyun.com (Y. Qiu).

https://doi.org/10.1016/j.ceramint.2018.06.119
Received 23 April 2018; Received in revised form 13 June 2018; Accepted 13 June 2018
0272-8842/ © 2018 Published by Elsevier Ltd.

Please cite this article as: Zhu, J., Ceramics International (2018), https://doi.org/10.1016/j.ceramint.2018.06.119

host/interlayer for Li-S batteries, the CNF-MnO demonstrates superior cycling stability, especially at high current density.

## 2. Experimental

### 2.1. Materials synthesis

Polyacrylonitrile (PAN) (average Mw = 150000), manganese acetate ($Mn(OAc)_2·4H_2O$, AR), N,N-Dimethylformamide (DMF) (anhydrous, 99.8%), sublimed sulfur powder (99.9%) are purchased from Aladdin Reagent Corporation Limited. Commercial porous carbon (CMK-3) is purchased from Nan Jing XFNANO Corporation Limited. All these materials are directly employed without further treatment. MnO NPs decorated carbon nanofibers (CNF-MnO) are fabricated by a facile electrospinning method. In a typical synthesis, 0.6 g of PAN and 0.18 g of $Mn(OAc)_2·4H_2O$ were firstly added into a small beaker and dissolved with 10 ml DMF solution. After stirring vigorously overnight, the electrospinning process is carried out for 10 h at room temperature by a conventional electrospinning system, during which the spinning parameters such as applied voltage, needle-to-collector distance, and flow rate are 13 kV, 18 cm, and 0.5 ml $h^{-1}$, respectively. After electrospinning, NFs are collected from graphite paper and subsequently stabilized in a tube furnace at 280 °C for 2 h in air followed by the calcination in nitrogen ($N_2$) ambiance at 1000 °C for 2 h (heating rate, 5 ° $min^{-1}$) to obtain the CNF-MnO nanocomposites. Similarly, the pure CNFs are also synthesized with the same experimental conditions.

The corresponding sulfur composites are fabricated with a melt diffusion method. Firstly, the CNF-MnO composite is grinded with sublimed sulfur (AR), with a weight ratio of 4:6 and preserved in a container with $N_2$ atmosphere and heat at 155 °C for 12 h in a vacuum system to get CNF-MnO-S composite. Similarly, the CNF with sulfur (CNF-S) composite and CMK-3 with sulfur (CMK-3-S) composite are also synthesized with the same method.

### 2.2. Material Characterization

X-ray diffraction (XRD, Model-Rigaku-D-Max-2500) is employed to confirm the crystal structure of the samples. The surface morphologies are examined by SEM (Model: HITACHI-S-4700) and TEM (Model: JEM-2010). The information about pore size and specific surface area was obtained by the BET and BJH methods. Thermogravimetric analysis (TGA) was applied at a constant rate of 5 °C $min^{-1}$ in air flow to evaluate the mass loading of C in the CNF-MnO, and in argon flow to evaluate the S content of CNF-MnO-S and CNF-S.

### 2.3. Electrochemical characterization

All electrochemical cells were assembled using CR2032 type coin cells. The S cathode was composed of active material, acetylene black (AB) and PVDF with a weight ratio of 7:2:1, and they are mixed with NMP solvent followed by stirring overnight. The mixed slurry is coated onto aluminium foil and dried in a vacuum furnace at 70 °C for 12 h. The areal mass loading of sulfur is about 1.0–1.4 mg $cm^{-1}$. The electrolyte was 1 M LiTFSI salt dissolved in DOL/DME (1:1, v/v) with 1% $LiNO_3$. The Li foil and Celgard-2400 membrane are used as the counter electrode and separators, respectively.

The galvanostatic discharge/charge tests were conducted with a LAND-CT-2001A battery tester within the voltage range of 1.7–2.8 V (vs. $Li/Li^+$). The cyclic voltammogram (CV) studies were carried out with a CHI-760D electrochemical workstation. Electrochemical impedance spectroscopy (EIS) studies were within a frequency range of 10 mHz-100 kHz.

In order to verify the absorption to LiPSs for CNF-MnO, a 5 mM of $Li_2S_4$ solution was prepared as typical polysulfides with a DME/DOL solvent as the electrolyte. Firstly, CNF-MnO ground with ball milling uniformly. After, 10 mg of CNF-MnO powder is dispersed into 3 ml of $Li_2S_4$ solution with a glass vial. Similarly, CNF powder and blank $Li_2S_4$ as the contrast samples are also measured with the above method. All samples are prepared in argon-filled glove box.

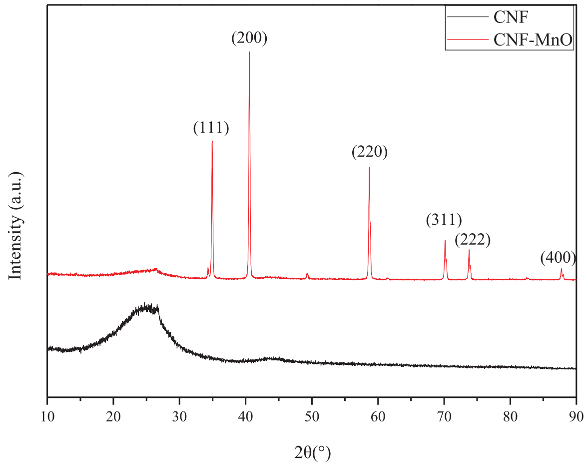

**Fig. 1.** XRD patterns of the CNF and CNF-MnO composites.

## 3. Results and discussion

In order to identify the crystal structure of the as-obtained CNF and CNF-MnO composites, XRD is employed as shown in Fig. 1. The XRD spectrum of CNF exhibits a broad diffraction peak at 26.4°. The diffraction peaks of CNF-MnO composites at 34.9°, 40.5°, 58.7°, 70.1°, 73.8° and 87.7° are indexed to the (111), (200), (220), (311), (222) and (400) planes, respectively of the manganosite phase of MnO (PDF 75–1090) with a little $Mn_3O_4$ (PDF 75-0765) phase. The broadening of the diffraction peaks indicates the small grain size with nano-scale for as-decorated MnO NPs. The TGA curves of the CNF-MnO and CNF-MnO-S are shown in Fig. S1. The carbon and MnO content in the CNF-MnO composite are 81.8 wt% and 19.2 wt%, respectively and the sulfur content in CNF-MnO-S is 60 wt%, which is in accordance with sulfur theoretical content.

The surface morphologies and particle distribution of the CNF-MnO and CNF-MnO-S composites are observed by SEM and TEM as shown in Fig. 2. Fig. 2a–b displays the SEM and TEM of CNF-MnO composite, in which the surface of the CNF-MnO is smooth and uniform with the diameter of 100 nm. Moreover, TEM results confirm the uniform distribution of the MnO NPs with the particle size of 5–20 nm throughout the carbon matrix (Fig. 2b, d–f). The low particle size of MnO may favour the $Li^+$ conduction. The small size of the CNF-MnO composites would accelerate the mobility of electron and Li ion so as to develop the utilization of sulfur. Information regarding the edge of MnO NPs is obtained with selected area electron diffraction (SAED) and indicates that the each MnO NPs are highly crystalline (Fig. 2c).

To further evaluate the specific surface area and pore size distribution of the pure CNF before and after MnO decoration, nitrogen adsorption-desorption measurements of CNF and CNF-MnO are conducted. As shown in Fig. S2a, $N_2$ absorption and desorption isotherms for CNF and CNF-MnO deliver obvious distinction. $N_2$ absorption and desorption isotherm of CNF own a typical characteristic for II-style isotherm, however, $N_2$ absorption and desorption isotherm of CNF-MnO belong to IV-style isotherm owing to the distribution of MnO NPs onto CNF. The CNF and CNF-MnO composites exhibited mesoporous nature (Fig. S2b). The BET surface areas of the CNF and CNFs-MnO composites are 91.4 $m^2$ $g^{-1}$ and 77.3 $m^2$ $g^{-1}$, respectively. The composite decorated with MnO NPs does not show obvious change in surface area but have a little difference for pore size to each other when compared with pure CNF. The average pore diameter of CNF and CNF-MnO are 43.9 and 53.3 nm, respectively. The MnO NPs that distributed uniformly

Download English Version:

https://daneshyari.com/en/article/7886181

Download Persian Version:

https://daneshyari.com/article/7886181

Daneshyari.com